STENTENNA: A MICROMACHINED ANTENNA STENT FOR WIRELESS MONITORING OF IMPLANTABLE MICROSENSORS

Kenichi Takahata, Andrew DeHennis, Kensall D. Wise, and Yogesh B. Gianchandani*
Department of Electrical Engineering and Computer Science, University of Michigan, Ann Arbor, USA

Abstract— **This paper reports on a micromachined stent that has been developed to serve as an antenna for wireless monitoring of implantable microsensors. A 4 mm long, 3.5 mm diameter design is fabricated from 50 µm thick stainless steel foil using a batch-compatible micro electro-discharge machining process. As it is expanded during deployment, the stent transforms from a mesh that fits snugly around the angioplasty balloon into an inductive coil. This is accomplished by strategically located breakable links which change its electrical characteristics during the plastic deformation into its final shape. This 20 nH coil is coupled to a capacitive pressure microsensor that is approximately 1.2 x1.4x0.5 mm³ in dimensions. Wireless monitoring is demonstrated by showing that the resonant electrical loading provided by this LC tank to a separate transmitting coil shifts by 400 KHz over a pressure change of 800 Torr. The tests are performed in a liquid environment.**

Keywords— **Stent, antenna, blood pressure, telemetry, micromachining**

I. INTRODUCTION

In recent years stents have come to play an essential role in the treatment of cardiovascular diseases. A stent typically has mesh-like walls in a tubular shape, and once positioned by a catheter, is expanded radially by the inflation of an angioplasty balloon. Its primary task is to physically expand and scaffold blood vessels that have been narrowed by plaque accumulation. Implantable pressure sensors are promising devices for chronic monitoring of blood pressure and flow rate, and could provide advance notice of restenosis, which is a common failure mechanism for stents.

Passive telemetric sensing of pressure has been demonstrated in the past, using a microchip with a planar thin film inductor fabricated together with a micromachined capacitive pressure sensor. This LC tank circuit to wirelessly loads down a separate, external transmitting coil [1]. The change in pressure can be detected by the shift in the frequency at which the external coil shows a characteristic dip in impedance.

This effort demonstrates a micromachined stent as an implantable antenna. The design that is presented is compatible with batch-manufacturable micro electro-discharge machining (µEDM) technology, and which automatically transforms the electrical characteristics of the stent during balloon angioplasty.

II. DESIGN & FABRICATION

Most commercially-available stents are made from laser-machined stainless steel tubes. It has recently been shown that stents cut from planar metal foils by µEDM in the fabrication offer very good mechanical properties [2]. These stents use flexural designs and do not have any bonded or welded seams. In assembling the device, a deflated angioplasty balloon is threaded alternately above and below a series of involute cross-bands between two longitudinal side beams, and then expanded by normal angioplasty procedure (Fig. 1). This design approach permits stents to be fabricated from steel foil with high throughput and precision by using planar electrodes as cookie-cutters that have been lithographically patterned on a silicon wafer [3]. However the final structure is essentially a set of series-connected rings which offers negligible inductance.

For a stent to serve as an antenna, its overall shape should follow the pattern of a helical coil (Fig. 2). However, the planar pattern of a helical coil does not provide sufficient mechanical robustness for subsequent handling during assembly and deployment. This challenge is addressed by inserting breakable links at select locations in the pattern (Fig. 2a). These links are created by narrowing the beam to create stress concentrations that ultimately fracture at certain locations when the balloon is inflated. Prior to balloon inflation, they provide the

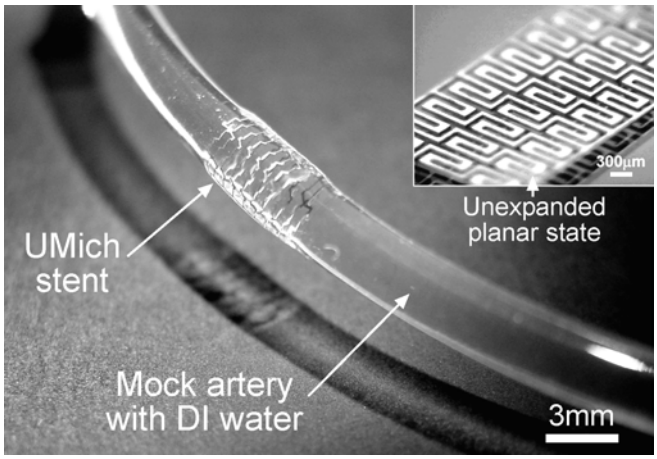

Fig. 1: Optical image of a UMich stent deployed inside a 3-mm diameter silicone mock artery with wall thickness of 0.25 mm using a standard angioplasty balloon catheter. Inset shows planar state of the stent prior to expansion.

* Contact information: 2405 EECS, 1301 Beal Avenue, Ann Arbor, MI 48108-2122, USA; Tel: 734-615-6407; Fax: 763-9324; Email: yogesh@umich.edu

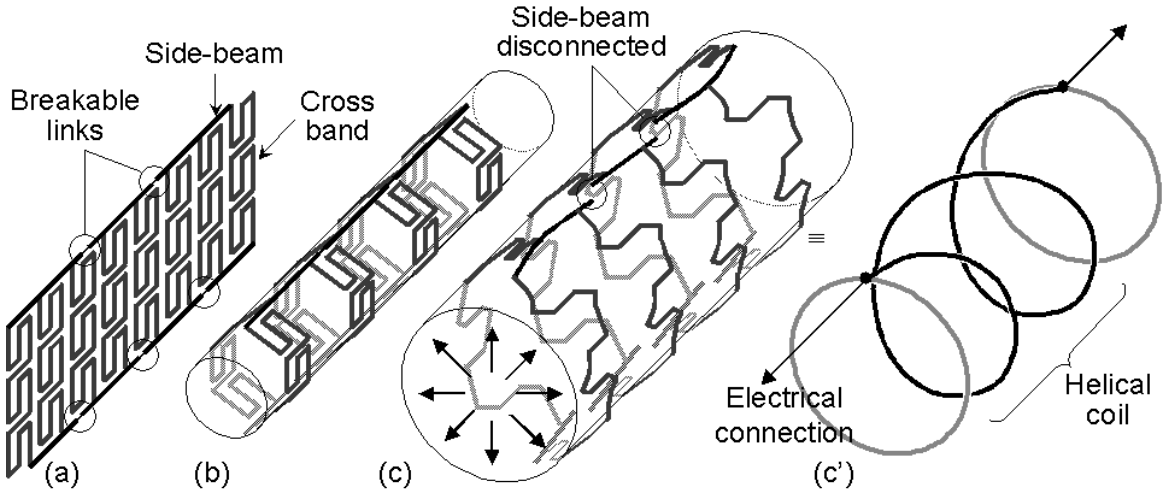

Fig.2: Stentenna formation: (a) A device in planar state, cut from 50-µm thick stainless steel foil using µEDM. Breakable links formed in side-beams by narrowing the width; (b) a deflated angioplasty balloon (not shown) is threaded into the device; (c) the device expanded by inflating balloon resulting in the links mechanically disconnected and a helical coil formed; (c') an electrical path (dark line) equivalent to the structure in (c).

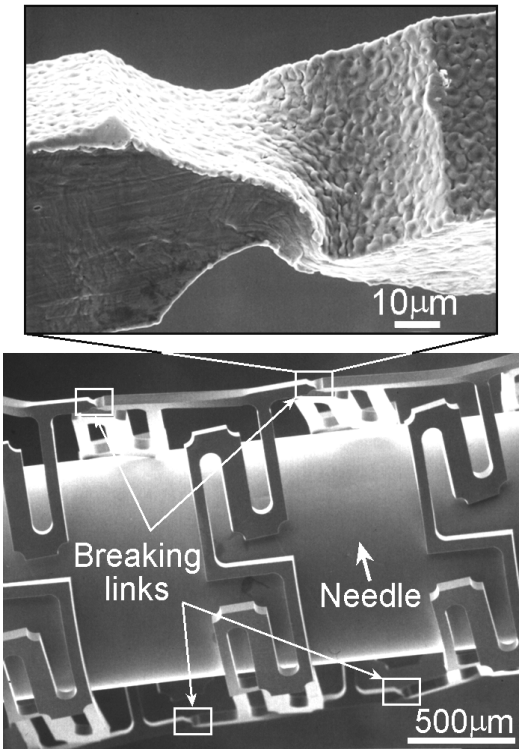

Fig. 3: (a-upper) A flexible link with narrowed width of 15 µm fabricated in a side-beam with 50-µm square cross section being plastically deformed; (b-lower) unbroken links in a pre-expanded stent.

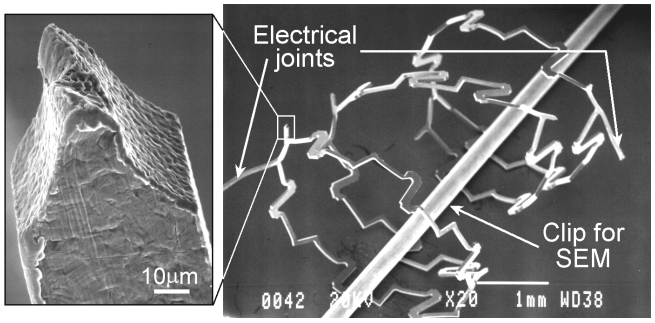

Fig. 4: (a-left) A broken link from an expanded stentenna; (b-right) the expanded stentenna.

mechanical strength to hold the structure (Fig. 2b) tightly around balloon during assembly and while it is being positioned with a catheter. When the balloon is expanded for deployment of the stent, torsional strain developed in the side-beams is effectively concentrated at the links (Fig. 3), leading to fracture, and resulting in a final shape that is essentially helical (Fig. 2c). Figure 4 shows a stentenna that was fabricated from 50 µm-thick type 304 stainless steel foil and expanded with a standard balloon catheter. (Note that although this particular sample has structural beams with a square cross section, they can be rounded by electrochemical polishing.) The length, diameter and number of turns are 4 mm, 3.5 mm, and 1.5 respectively in this sample. Its measured inductance changes from an undetectable level to 20 nH upon expansion.

For an effective wireless link, minimal damping is desired in the LC tank. The quality factor is expressed as:

$$Q \approx \frac{1}{R_{STp}} \sqrt{\frac{L_{ST}}{C_{SE} + C_{STp}}} \qquad (1)$$

where L_{ST} is inductance of the stentenna, C_{SE} is capacitance of the sensor, C_{STp} is parasitic capacitance, and R_{STp} is parasitic resistance. The impact of the R_{STp} is greater than that of C_{STp}. The parasitic resistance contributed by stentenna is inversely related to the beam corss-section, whereas the parasitic capacitance that it contributes is proportional to the beam surface area. Therefore, R_{STp}

depends on the square of the beam diameter whereas C_{STp} is simply proportional to it. Thus, it is electrically favorable to increase the thickness of the beams. In fact, this is favorable mechanically as well, because it would increase the radial stiffness of the stent. However, from the biological viewpoint, increasing the volume of the structural elements can be undesirable, which may warrant application-specific designs and structural optimization.

The micromachined pressure sensor that was used in this effort consisted of a vacuum-sealed cavity capped by a 3.7-μm thick p^{++} Si circular diaphragm with the 1-mm diameter and 5-μm gap [4]. The diaphragm had a 10-μm thick boss with varied diameter for providing different dynamic range and an oxide layer on the backside for electrical protection in case of a contact between the diaphragm and a bottom electrode (Fig. 5a). The sensors were fabricated by a silicon-on-glass dissolved wafer process. The fabrication was combined with a reflowed Si-Au eutectic bonding technique for achieving low-impedance interconnect (Ti:50 nm/Pt:80 nm/Au:150 nm) to the sealed sensor (Fig. 5b).

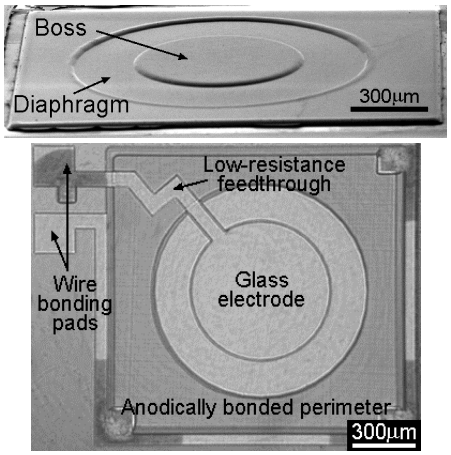

Fig. 5: (a-upper) An SEM image of the pressure sensor; (b-lower) an optical image of a pressure sensor taken through the glass substrate after bonding.

III. EXPERIMENTAL RESULTS

The stentenna was tested and characterized for both electrical and mechanical response. The electrical tests were performed under both dry and wet conditions: (A) in air below atmospheric pressure; and (B) in liquid elevated pressures comparable to those encountered in arteries. A non-conductive liquid was used in these preliminary measurements. The test set-up is illustrated in Fig. 6, in which the stentenna was connected in parallel to the capacitive pressure sensor, both located in a pressure-controlled chamber. Figure 7 plots a response of capacitance in a pressure sensor. The pressure was varied as the input impedance Z_{in} of the external coil was monitored with an HP 4195 spectrum analyzer. The elements used in each experiment are described in Table I. For the dry measurements (condition A), a self-resonant peak in Z_{in} –

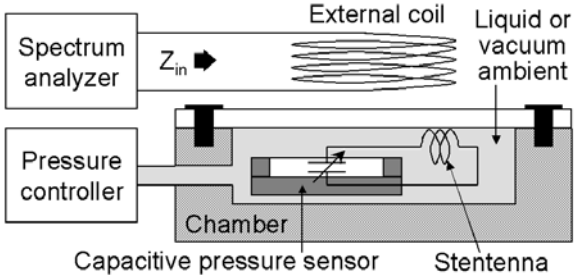

Fig. 6: A wireless set-up for monitoring a capacitive pressure sensor using a stentenna.

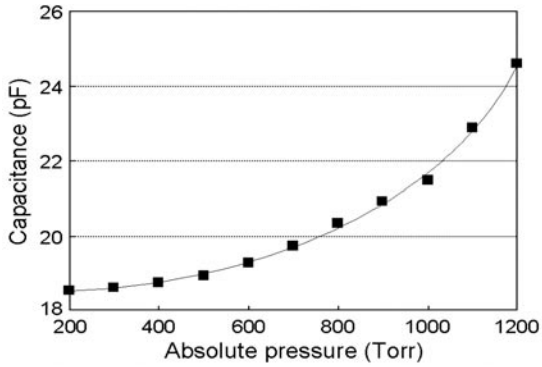

Fig. 7: Capacitance of the sensor which was used in the dry test as a function of pressure.

TABLE I
CHARACTERISTICS OF ELEMENTS USED IN WIRELESS TESTS

Test	Pressure sensor (at 760 Torr)		Primary/external coil	
	Capacitance	Sensitivity	Diameter	Inductance
(A)	20 pF	5.4 fF/Torr	20 mm	1.5 μH
(B)	17 pF	5.0 fF/Torr	10 mm	0.3 μH

located nominally at 57.7 MHz – shifted by +170 KHz as the pressure changed by -615 Torr (Fig. 8a). Despite a relatively noisy signal, the shift in peaks could be easily resolved because the measured *Q* of the resonant peak was about 115. Figure 8b plots the dependence of the resonant frequency on the pressure and demonstrates an approximately linear response of 274 Hz/Torr. The nominal resonant frequency in the wet tests under condition (B) was 201 MHz. This differed from case (A) because different primary coil was used. The frequency was shifted by -760 KHz with pressure change of +1380 Torr (Fig. 9a). The pressure response was 500 Hz/Torr in this case (Fig. 9b).

The experimental results were evaluated using SPICE™. Figure 10a illustrates an equivalent circuit model for the wireless setup for the dry set-up (A). In the model, L_{EX}, L_{ST}', and k denote inductance of an external coil, lumped inductance of stentenna and interconnect, and coupling coefficient respectively. Other elements were measured or fitted parasitics. The simulation result shown in Fig. 10b indicated that a capacitance change ΔC_{SE}=-1.2 pF in the pressure sensors, corresponding to a -500 Torr shift from 700 Torr in absolute pressure caused a +137 KHz shift in the resonant frequency of Z_{in}, which is comparable to the measurements.

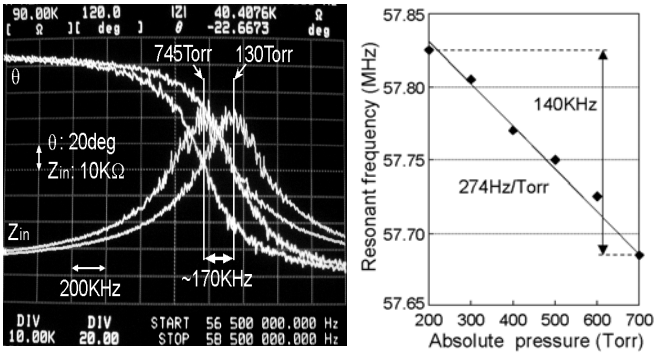

Fig. 8 Measurement result with air ambient: (a-left) Impedance Z_{in} and phase θ in the external coil shows the resonant frequency shifted by +170 KHz due to a pressure change of -615 Torr; (b-right) pressure response of the resonant frequency.

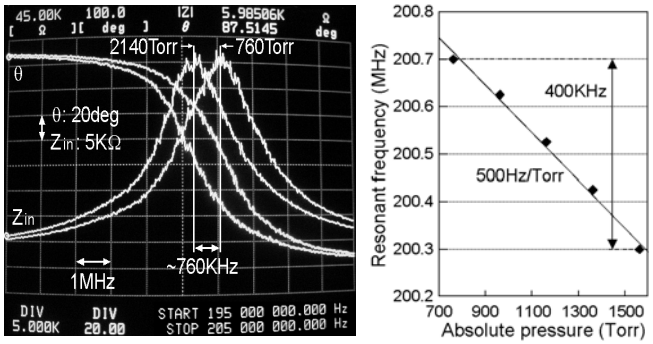

Fig. 9: Measurement result with liquid ambient: (a-left) Resonant frequency of Z_{in} shifted by -760 KHz due to a pressure change of +1380 Torr; (b-right) pressure response of the resonant frequency.

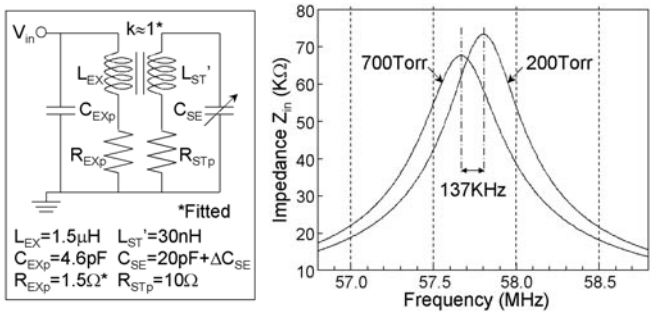

Fig. 10: (a-left) Circuit model used in SPICE™ analysis; (b-right) simulation showing the shift in the resonant peak of the impedance Z_{in} of the external coil.

A mechanical loading test was performed for assessing radial strength of the stentenna. A 4-mm long sample was clipped on a z-stage and compressed radially by a micrometer against a fixed force gauge (Imada DPS-1) as shown in Fig. 11a. The measured response showed elastic behavior over a deflection range of 400 μm and a stiffness of 225 N/m (Fig. 11b). While the radial strength of this stent has been somewhat compromised compared to the best designs reported in [2], it is worth noting that, at 50 μm, the thickness of the steel foil used for these devices is half that used for many commercial stents, so it is easy to increase.

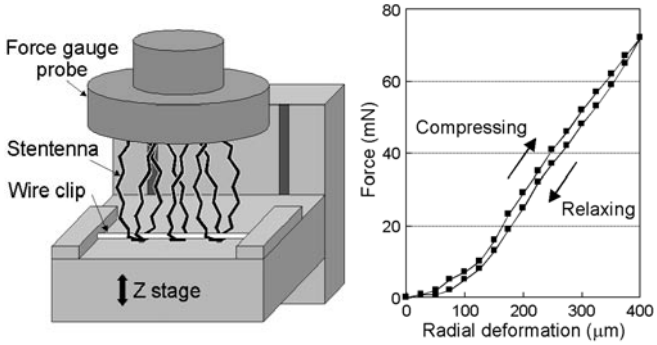

Fig. 11: (a-left) A set-up for the radial strength test; (b-right) reaction force of a 4-mm long stentenna measured in the test.

IV. CONCLUSION

Wireless acquisition of pressure has been demonstrated using a micromachined stentenna with a capacitive pressure sensor, validating the concept of using stents as antennas for microsensors. A 20 nH stentenna with 4-mm length, 3.5-mm diameter and 50-μm thickness was coupled to a capacitive pressure sensor with dimensions of $1.2 \times 1.4 \times 0.5\ mm^3$ and sensitivity of 5 fF/Torr. A new design and fabrication method was demonstrated for the stentenna, exploiting the use of strategically placed breakable links that were severed by stress concentrations during inflation of the angioplasty balloon. This design and fabrication method may also be extended to other micromachined components such 3D coils and transformers for RF communication. Telemetrically powered implantable devices, such as the muscular stimulator reported in [5] and the neural recoding system sensor reported in [6], may also benefit from this technology.

ACKNOWLEDGMENTS

The exploration of micro-discharge based manufacturing is supported in part by a grant from the National Science Foundation. The portion of this work associated with pressure sensors is supported by the Engineering Research Centers Program of the National Science Foundation under Award Number EEC-9986866 and by a gift from Ms. Polly Anderson.

REFERENCES

[1] A. DeHennis, K.D. Wise, A Double-Sided Single-Chip Wireless Pressure Sensor, *Proc. IEEE MEMS Conf.* 2002, pp. 252-5

[2] K. Takahata, Y.B. Gianchandani, Coronary Artery Stents Microfabricated from Planar Metal Foil: Design, Fabrication, and Mechanical Testing, *Proc. IEEE MEMS Conf.*, 2003, pp. 462-5

[3] K. Takahata, Y.B. Gianchandani, Batch Mode Micro-Electro-Discharge Machining, *IEEE J. MEMS*, 11(2), 2002, pp.102-110

[4] A. DeHennis, K.D. Wise, An All-Capacitive Sensing Chip for Temperature, Absolute Pressure, and Relative Humidity, *Proc. IEEE Transducers*, 2003 (to be published)

[5] B. Ziaie, M.D. Nardin,, A.R. Coghlan, K. Najafi, A Single-Channel Implantable Microstimulator for Functional Neuromuscular Stimulation, *IEEE Trans. Biomed. Eng.*, 44(10), 1997, pp. 909 -920

[6] T. Akin, K. Najafi, R.M. Bradley, A Wireless Implantable Multichannel Digital Neural Recording System for A Micromachined Sieve Electrode, *IEEE J. Solid-State Circuits*, 33(1), 1998, pp. 109 -118